Organic Process Research & Development **2006**, *10,* 278–284

Continuous Hydrogenation of 2-Butyne-1,4-diol to 2-Butene- and Butane-1,4-diols

C. V. Rode,* P. R. Tayade, J. M. Nadgeri, R. Jaganathan, and R. V. Chaudhari
Homogeneous Catalysis Division, National Chemical Laboratory, Dr. Homi Bhabha Road, Pune - 411008, India

Abstract:

Continuous catalytic hydrogenation of 2-butyne-1,4-diol (B_3D) was carried out in a fixed-bed reactor over 1% $Pt/CaCO_3$ catalyst to give 2-butene-1,4-diol (B_2D) and butane-1,4-diol (B_1D) without formation of any other side products. In case of continuous hydrogenation, higher selectivity (66%) to B_2D could be obtained and the selectivity pattern was completely different from that found in case of batch slurry operation in which B_1D selectivity was very much higher (83%) than the B_2D selectivity (17%). Another interesting feature was that by varying the contact time, the selectivity to both B_2D as well as B_1D could be varied over a wide range which is an attractive option to obtain the desired products mix of B_1D and B_2D, depending on the fluctuation in the market demand. Further, a mathematical model for reactor performance was also developed on the basis of the kinetic data obtained previously in a batch slurry reactor. The predicted values of conversion, selectivity, and rate of hydrogenation were found to agree with the experimental data over a wide range of conditions.

Introduction

Hydrogenation B_3D in the presence of a catalyst is an industrially important reaction for the manufacture of B_2D and B_1D.[1] The olefinic diol, B_2D, is a starting material for the manufacture of endosulfan and vitamins A and B_6, whereas B_1D has a wide range of applications in the polymer industry and as a raw material for the manufacture of tetrahydrofuran.[1−3] The earlier processes described Ni- and Cu-based catalysts for butyne diol hydrogenation under severe operating conditions (15−30 MPa H_2 pressure and up to 433 K temperature).[4] The noble metals such as palladium, ruthenium alone or in combination with other metals such as zinc, lead, cadmium, copper, and/or organic amines also were used as catalyst systems to improve selectivity (ratio of concentration of desired product formed to the concentration of substrate consumed) to the intermediate, B_2D.[1,5−8] A monometallic Pd/C catalyst was reported to give 60−70% selectivity to B_2D while remaining is a mixture of saturated diol (B_1D) along with other side products such as γ-hydroxy butyraldehyde, *n*-butyraldehyde, *n*-butanol, crotyl alcohol, and acetal due to the double bond migration and hydrogenolysis of B_2D in the presence of a catalyst.[4,5] It is clear from the literature that, for butyne diol hydrogenation, a monometallic catalyst system gives saturated diol (B_1D) as major product along with other side products, whereas a combination of two or more metals or the presence of organic/inorganic bases gives enhanced selectivity to B_2D; however, such catalyst systems lack consistency in activity in subsequent catalyst reuse, and moreover, such processes require the complete removal of the additives for obtaining highest purity of the product for its end use in the fine chemical or pharmaceutical sector. Also, previous work on butynediol hydrogenation has mainly been carried out in a batch slurry reactor using finely powdered catalyst in which the selectivity ratio of B_2D to B_1D is normally constant. Since both B_2D and B_1D are large-scale commercial products, it would be most desirable to have a continuous hydrogenation of B_3D to give either B_2D or B_1D selectively or a desired mixture of B_2D and B_1D. As per the market demand, this continuous operation for the hydrogenation of B_3D by merely changing the operating conditions can give a desired mixture of B_2D and B_1D (Figure 8) for the same catalyst. Hence, objectives of this work were (i) to investigate the activity and selectivity of 1%$Pt/CaCO_3$ catalyst for continuous hydrogenation of butyne diol in a fixed-bed reactor, (ii) to study the effect of various reaction parameters on the conversion and selectivity behaviour for the continuous hydrogenation of B_3D, and (iii) to develop a reactor model that provides reasonably accurate conversion and selectivity predictions for various reactor inlet conditions. For this purpose, hydrogenation of butyne diol was carried out in a tubular reactor (30 g capacity); we found that the selectivity pattern obtained in a fixed-bed reactor was different from that obtained in the slurry reactor at similar conversion levels and that the selectivity ratio of B_1D to B_2D could be altered by varying the H_2 pressure, temperature, liquid and and gas flow rate conditions at the reactor inlet. The predictions obtained by the proposed reactor model were compared with the experimental data and were found to agree well over a wide range of operating conditions.

Experimental Section

Materials. B_3D of >99.5% purity was obtained from E.Merck India, Ltd., and 10% aqueous solution was used.

* To whom correspondence should be addressed. Fax: +91 20 25893260. E-mail: cv.rode@ncl.res.in.

(1) Winterbottom, J. M.; Marwan, H.; Viladevall, J.; Sharma, S.; Raymashasay, S.; Heterogeneous catalysis and fine chemicals IV. In Blaser, H. V., Baiker, A., Prins, R., Eds.; *Stud. Surf. Sci. Catal.* **1997**, *108*, 59.
(2) Chaudhari, R. V. In *Proceedings of the Indo- German Workshop on High-Pressure Technology Engineering*; Chaudhari, R. V., Hofmann H., Eds.; Forschungszentrum Julich GmbH: Germany, 1993; p 197.
(3) Telkar, M. M.; Rode, C. V.; Rane, V. H.; Jagannthan, R.; Chaudhari, R. V. *Appl. Catal., A* **2001**, *216*, 13.
(4) Rylander, P. N. In *Hydrogenation Methods*; Katrizky, A. R., Methcohn, O., Rees, C. W., Eds.; Academic Press: New York, 1985.
(5) Bond, G. C.; Webb, G.; Winterbottom, J. M. *J. Catal.* **1962**, *1*, 74.
(6) Rosso, R.; Mazzocchia, C.; Gronchi, P.; Centola, P. *Appl. Catal.* **1984**, *9*, 269.
(7) Fukuda, T.; Kusama, T. *Bull. Chem. Soc. Jpn.* **1958**, *31*, 339.
(8) Bollger, G.; Boer, W.; Wache, H.; Gratze, H.; Koerning, W.; Ger. Pat. 2451929, 1976.

Published on Web 02/16/2006
10.1021/op050216r CCC: $33.50

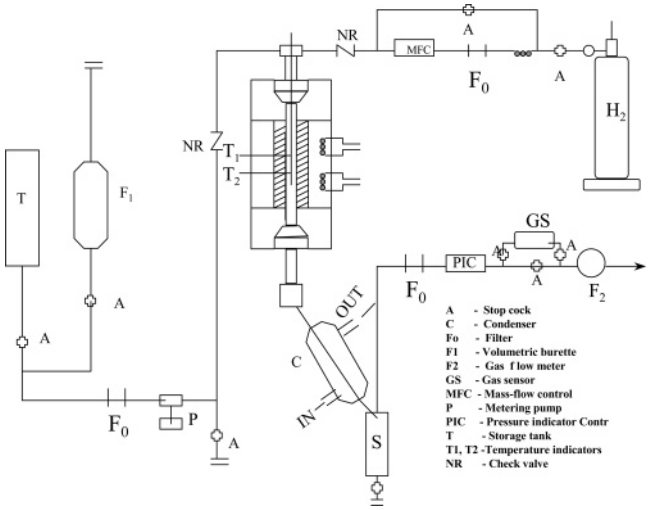

Figure 1. **A schematic of the trickle-bed reactor setup.**

Hydrogen gas with >99.98% purity was supplied by M/s Indian Oxygen Ltd., Mumbai, and was used directly from the cylinder. For the preparation of 1%Pt/$CaCO_3$ catalyst, the required quantity of $PtCl_4$ was dissolved in minimum amount of water; if necessary, a small quantity of dilute HCl was added to ensure the complete dissolution of the precursor. Under stirring, the slurry of support prepared in water was added to the above solution, and temperature was maintained at 353 K. After 1 h, formaldehyde was added under stirring. Then the reaction mixture was cooled, filtered to obtain the catalyst, which was then dried at room temperature under vacuum. The powdered catalyst was then pelletized in the form of pellets of 4-mm diameter.

Fixed-Bed Bench Scale Reactor Setup. All the hydrogenation experiments were carried out in a bench scale, high-pressure, fixed-bed reactor supplied by M/s Geomechanique, France. A schematic of the reactor setup is shown in Figure 1. It consisted of a stainless steel tube of 0.35 m length and 1.5×10^{-2} m inner diameter that was heated by two tubular furnaces whose zones (TIC1 and TIC2) were independently controlled at the desired bed temperature. The reactor was provided with two thermocouples [Chromel-Alume thermocouples (type K)] to measure the temperature at two different points. The reactor was equipped with mass flow controllers, pressure indicator, and controller (PIC) devices. A storage tank was connected to the metering pump through a volumetric buret to measure the liquid flow rate. The pump had a maximum capacity of 3×10^{-4} m^3/h under a pressure of 10 MPa. The other end of the reactor was connected to a gas−liquid separator through a condenser.

The experiments were carried out over 10 and 20 g of catalyst in the form of pellets having 4 mm diameter. The section 5 cm above and 5 cm below the catalyst bed was packed with inert packing (carborundum), thus providing the catalyst bed depth of ~0.25 m. The reactor was flushed thoroughly with H_2 at room temperature before the start of the actual experiment. After attaining the desired temperature the reactor was pressurized with H_2. The liquid feed was "switched on" after the reactor has reached the operating pressure and kept there for 1 h to obtain the constant liquid flow rate. Liquid samples were withdrawn at regular intervals

Table 1. **Range of operating conditions**

catalyst	1% Pt/$CaCO_3$
initial concentration of B_3D	1.16 kmol/m^3
solvent	water
H_2 pressure	10−70 bar
liquid velocity, U_l	10−60 mL/h
gas velocity, U_g	20−80 NL/h
reactor diameter (i.d.)	0.015 m
total reactor length	0.35 m
catalyst packing length	0.25 m
bed voidage	0.7
particle diameter, d_p	0.004 m
density of the catalyst, ρ_p	1685 kg/m^3
porosity of the catalyst, ϵ	0.1050
tortosity of the catalyst, τ	6.2

Scheme 1. **Hydrogenation of B_3D**

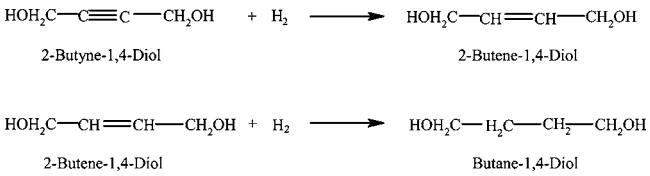

of time and were analyzed by gas chromatography (HP 6890 series) o.d. 0.32 m, helium gas as carrier, FID detector, operating temp 80−190 °C using HP-FFAP capillary column.

The liquid velocity was changed after confirming the steady-state achievement. Following this procedure, the experiments were carried out at different inlet conditions of liquid flow rate, gas flow rate. The reactor was operated in the temperature and pressure ranges of 60−100 °C and 10−70 bar respectively. The steady state performance of the reactor was observed by analysis of the reactant and products in the exit stream.

Results and Discussion

The main objectives of this work were (i) to investigate the activity and selectivity behaviour of 1%Pt/$CaCO_3$ catalyst for continuous hydrogenation of B_3D in a fixed-bed reactor, (ii) to study the effect of various reaction parameters on the conversion and selectivity behaviour for the continuous hydrogenation of B_3D, and (iii) to develop a reactor model for predicting the conversion and selectivity under various inlet conditions. For this purpose, the effects of temperature, H_2 pressure, liquid and gas flow rates, catalyst loading on the conversion of B_3D and the product selectivities were investigated. The range of reaction conditions is given in Table 1. In all experiments, the concentrations of the reactants and products in the reactor effluent were determined from which the conversion and selectivity were calculated. The material balance as per the reaction Scheme 1, was found to be in the range of 98−100% in all the experiments. Reproducibility of the rate, conversion, and selectivity measurements was found to be within 3−4% error as indicated by a few repeated experiments. The results are discussed below.

For 1%Pt/$CaCO_3$ catalyst, the products of B_3D hydrogenation were B_2D and B_1D as per the reaction Scheme 1. Table 2 shows the variation of conversion and selectivity as a function of contact time defined as a ratio of catalyst

Table 2. **Activity and selectivity pattern for butyne diol hydrogenation in a fixed-bed reactor**

sr. no.	*W*/*F* (h)	conversion (%)	selectivity %	
			B_1D	B_2D
1	0.33	14	34	66
2	0.50	30	42	58
3	0.66	40	49	51
4	1.11	55	59	41
5	2	78	73	27

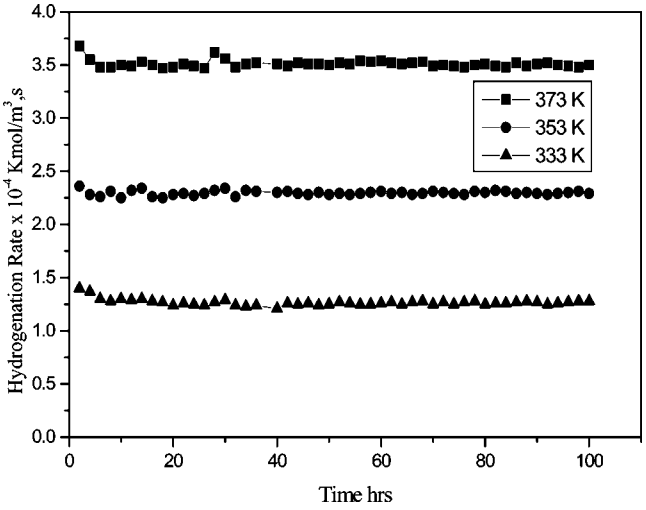

Figure 2. **Time on stream catalyst activity profile. Reaction conditions: pressure, 20 bar; gas flow rate, 20 L/h; liquid flow rate, 20 mL/h; catalyst weight, 20 g.**

loading to the liquid flow rate (*W*/*F*, h). Obviously, the conversion of B_3D increased with increase in contact time. The selectivity pattern was completely different from that found in case of batch slurry operation in which B_1D selectivity was very much higher (83%) than the B_2D selectivity (17%).[9] As can be seen from Table 2, varying the contact time at different conversion levels could vary the selectivity to both B_2D as well as B_1D over a wide range. This is an attractive option for a commercial operation where the desired products mix of B_1D and B_2D can be achieved, depending on the fluctuation in the market demand.

Some preliminary experiments showed that the activity of 1%Pt/$CaCO_3$ for the hydrogenation of B_3D was constant for >100 h in the temperature range of 333−373 K (Figure 2), confirming the uniform activity for the duration of all experiments carried out in this work. Therefore, all of the data collected for the purpose of reactor modeling and reactor performance studies were under steady-state conditions.

Effect of Liquid Flow Rate. The effect of liquid flow rate on conversion of B_3D was studied in the range of 10−60 mL/h, under constant temperature, H_2 pressure, and gas flow rate conditions, and the results are shown in Figures 3 and 4. The conversion of B_3D decreased almost proportionately (from 70 to 12%) with increase in liquid flow rate from 10 to 60 mL/h (see Figure 3). One of the main reasons for decrease in the conversion is that, as the liquid flow rate

(9) Telkar, M. M.; Rode, C. V.; Jagannthan, R.; Rane, V. H.; Chaudhari, R. V. *J. Mol. Catal. A: Chem*. **2002**, *187*, 81.

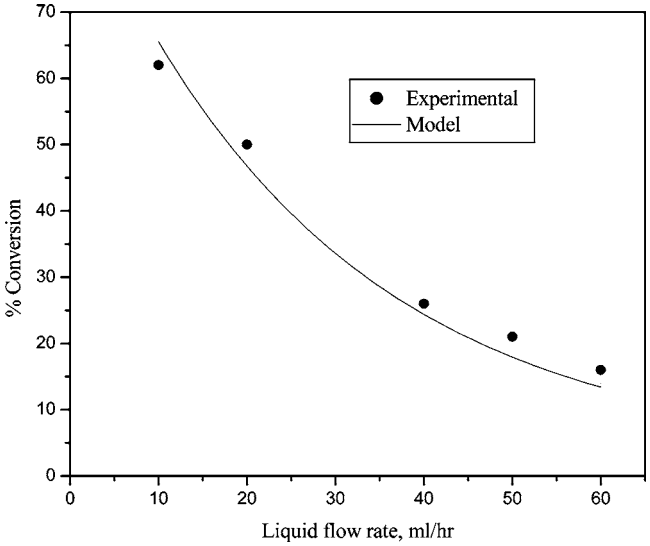

Figure 3. **Effect of liquid flow rate on conversion. Reaction conditions: p_{H2}, 20 bar; H_2 flow rate, 20 L/h; temperature, 100 °C; catalyst weight, 10 g.**

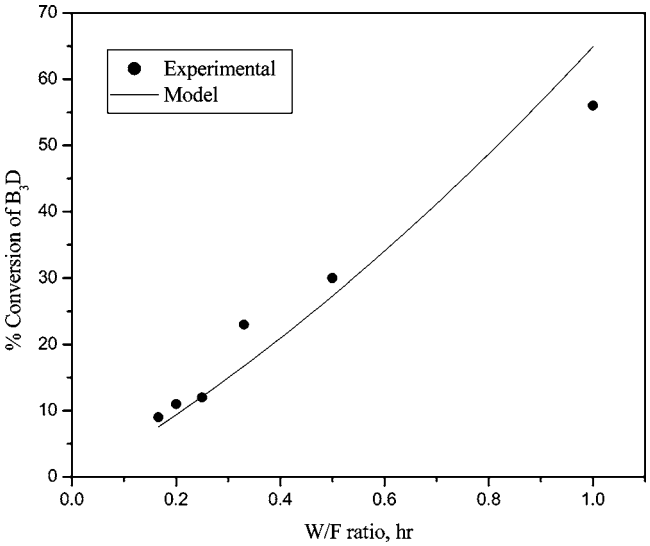

Figure 4. **Effect of liquid flow rate on conversion. Reaction conditions: pressure, 20 bar; H_2 flow rate, 20 L/h; temperature, 100 °C; catalyst weight, 20 g.**

was increased, the residence time of B_3D in the reactor was reduced and less time was available for the intimate contact of H_2 with liquid B_3D and with the catalyst pellets; thus, proper diffusion was not possible. Another reason is that, although the increase in the liquid flow rate could wet more surface area of catalyst pellets and there was an increase in the gas−liquid and liquid−solid mass transfer coefficient, at lower liquid velocity, catalyst particles were partially wetted; under these conditions the rate would increase due to direct transfer of the gas-phase reactant to the catalyst surface (already wetted internally due to capillary forces). Hence, with an increase in the liquid flow rate, an increase in the wetted fraction was expected to retard the rate of reaction.[10,11] The overall rate of hydrogenation (Figure 5) decreased with increase in the liquid flow rate. In the range of 10−25 mL/h liquid flow rate, the fall in the rate is fast, and eventually it becomes slower. The model predictions for the effect of liquid flow rate on the conversion and overall

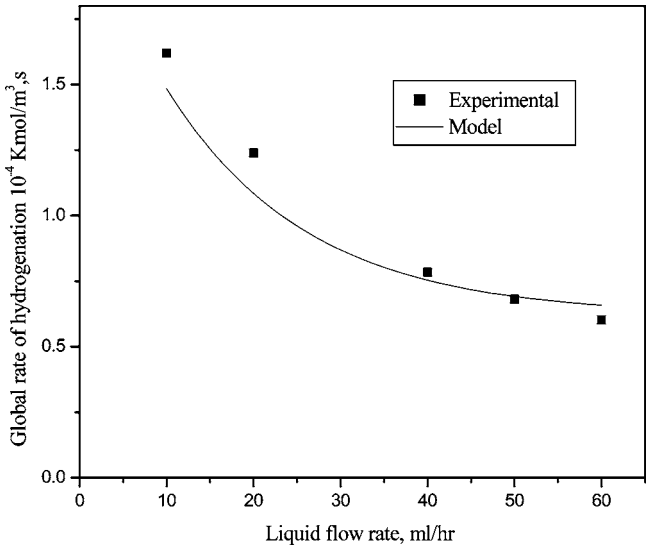

Figure 5. **Effect of liquid flow rate on rate of hydrogenation. Reaction conditions: pressure, 20 bar; H_2 flow rate, 20 L/h; temperature, 100 °C; catalyst weight, 20 g.**

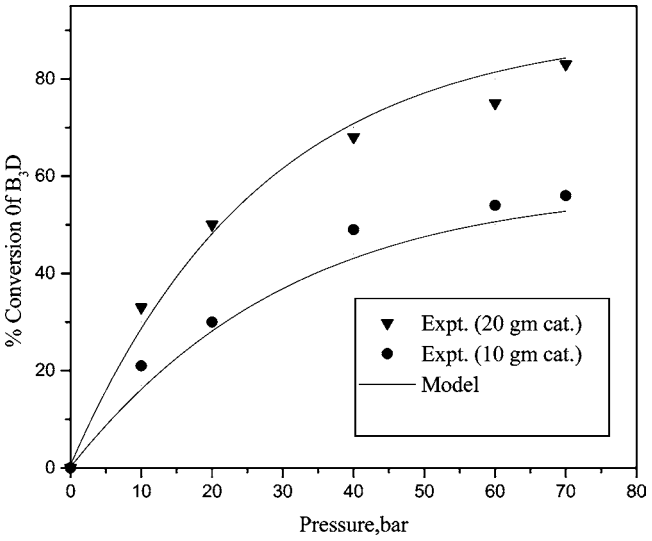

Figure 6. **Effect of H_2 pressure on conversion. Reaction conditions: liquid flow rate, 20 mL/h; H_2 flow rate, 20 L/h; temperature, 100 °C.**

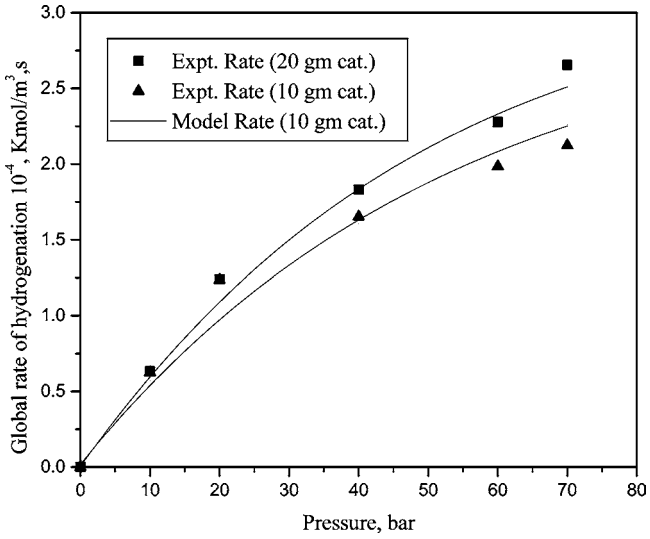

Figure 7. **Effect of hydrogen pressure on rate of hydrogenation.Reaction conditions: liquid flow rate, 20 mL/h; H_2 flow rate, 20 L/h; temperature, 100 °C.**

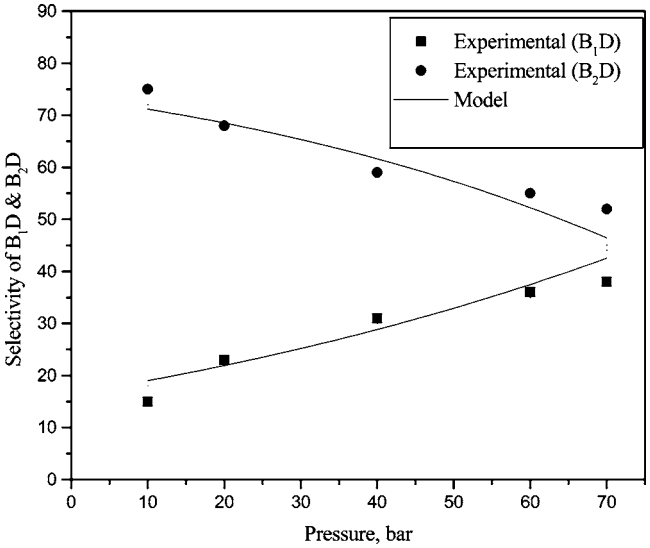

Figure 8. **Effect of hydrogen pressure on the selectivity of B_2D and B_1D. Reaction conditions: liquid flow rate, 20 mL/h; catalyst weight, 20 g; H_2 flow rate, 20 L/h.**

rate of hydrogenation are in well agreement with the experimental results (see Figures 3 and 5).

Effect of H_2 Pressure. The effect of hydrogen pressure on the conversion of B_3D was studied in the range of 10−70 bar H_2 pressure for 10 and 20 g of catalyst loadings and at 100 °C, and the results are shown in the Figure 6. Initially, B_3D conversion increased almost linearly with increase in pressure up to 40 bar H_2 pressure. The overall rate of hydrogenation was also found to increase with increase in H_2 pressure (Figure 7) for both the catalyst loadings. The increase in H_2 pressure increases the gas−liquid and liquid−solid mass transfer coefficient, leading to higher conversion and hydrogenation rates. It was interesting to note that with increase in H_2 pressure, the selectivity patterns of B_2D and B_1D were exactly opposite to each other (see Figure 8). In the lower range of H_2 pressure (10−40 bar), the difference between the selectivities of B_2D and B_1D was larger; eventually, 50:50 formation of B_2D and B_1D could be obtained at 70 bar H_2 pressure. The predictions of the model equations for the effect of pressure on the conversion of B_3D, selectivity of B_2D and B_1D, and overall rate of hydrogenation is in good agreement with the experimental results.

Effect of Hydrogen Flow Rate. The effect of hydrogen gas flow rate on conversion of B_3D and selectivities of B_2D and B_1D were studied in the range of 20−80 L/h at constant pressure, temperature, and liquid flow rate conditions. The conversion of B_3D was slightly lower at the lower and higher gas flow rates as compared with that in the middle range (Figure 9). The reason for this situation is that at lower gas flow rate the gas cannot overcome the gas−liquid mass transfer resistance, while at higher gas flow rates, although the gas reduces the liquid film thickness around the catalyst

(10) Malyala, V.; Rajashekharam, Jagannthan R.; Chaudhari, R. V. *Chem. Eng. Sci.* **1998**, *53*, 787.
(11) Chaudhari, R. V.; Jagannthan, R.; Mathew, S. P. *AIChE J.* **2002**, *48*, 110−125.

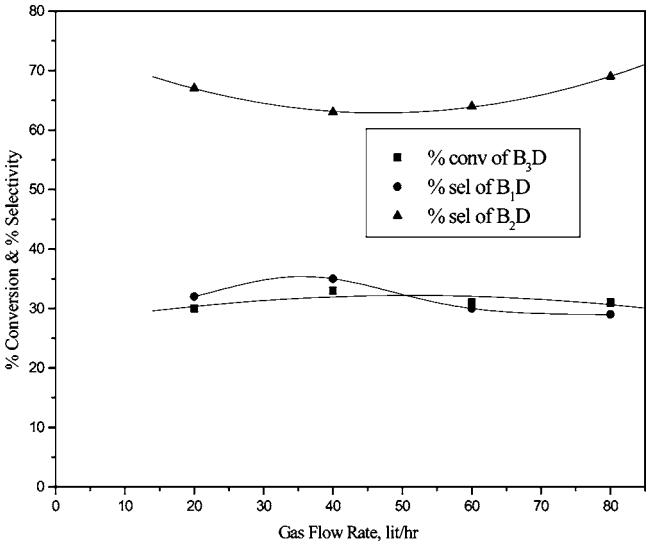

Figure 9. **Effect of gas flow rate on conversion of B_3D. Reaction conditions: liquid flow rate, 20 mL/h; H_2 pressure, 20 bar; temperature, 100 °C; catalyst weight, 10 g.**

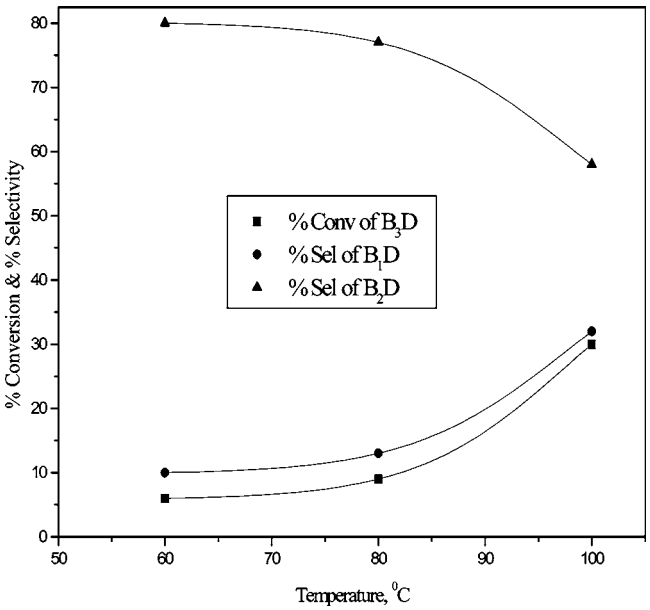

Figure 10. **Effect of temperature on conversion of B_3D and selectivity of B_1D and B_2D. Reaction conditions: liquid flow rate, 20 mL/h; H_2 flow rate, 20 L/h; pressure, 20 bar; catalyst weight, 10 g.**

pellets, the gas phase becomes continuous, and the liquid phase becomes dispersed. With further increase in gas flow rate, the flow regime changes to spray flow regime, and this causes greater velocities in the liquid phase by increasing the drag forces on the liquid phase. The selectivities to both B_2D and B_1D were nearly constant since the change in gas flow rate did not affect the intrinsic reaction kinetics to a considerable extent.

Effect of Temperature. The effect of temperature on conversion of B_3D and selectivity patterns of B_2D and B_1D were studied by varying the temperature from 60 to 100 °C (Figure 10). The conversion increased from 5 to 30% with increase in temperature from 60 to 100 °C since, the temperature has a greater impact on the reaction kinetics. The selectivity patterns of B_1D and B_2D showed opposite trends with an increase in temperature, obviously because at higher temperature B_2D gets converted to the saturated diol B_1D.

Table 3. **Kinetic parameters for the hydrogenation of B_3D**

	rate constants $((m^3)^2/kmol\ kg{\cdot}s)$		adsorption constants $(kmol/m^3)$	
temp (K)	k_1	k_2	K_B	K_C
333	1.940	1.210	8.101	2.11
343	3.178	2.790	9.80	2.60
353	5.037	6.140	11.728	3.183
363	7.802	12.934	13.898	3.843
373	11.804	26.178	16.32	4.594

Reactor Modeling. A trickle-bed reactor model for the hydrogenation of B_3D was developed using the rate equations proposed by Telkar et al. based on the rate data in a slurry reactor to represent the intrinsic kinetics for different reaction steps as shown in Scheme 1.[9]

$$r_1 = \frac{wk_1A^*B_l}{(1 + K_BB_l + K_cc_l)^2} \quad (1)$$

$$r_2 = \frac{wk_2A^*C_l}{(1 + K_BB_l + K_cc)^2} \quad (2)$$

The overall rate of hydrogenation can be given as

$$R_A = \frac{wk_1A^*(B_l + k_{21}C_l)}{(1 + K_BB_l + K_cc)^2} \quad (3)$$

where A, B_l, and, C_l represent the concentrations of H_2, B_2D, and B_1D. A nonlinear least-squares regression analysis was used to obtain the values of the kinetic parameters in the above rate equation. For this purpose an optimization program based on the Marquardt's method[12] was used. The different kinetic parameter values evaluated for the above rate equation are given in Table 3.

To develop a trickle-bed reactor model applicable to hydrogenation of B_3D, the approximate solution of the catalytic effectiveness factor was performed for partial wetting of catalyst particles.[13] The overall catalyst effectiveness factor could be expressed as a sum of the weighted average of the effectiveness factor in the dynamic liquid-covered, stagnant liquid-covered and complete gas-covered zones and with the assumptions that (a) gas and liquid phases are in plug flow; (b) the liquid-phase reactant is nonvolatile and was in excess as compared to the gaseous reactant; (c) the gas−liquid, liquid−solid, and intraparticle mass transfer resistances for H_2 are considered, whereas the liquid−solid and intraparticle mass transfer resistances for the liquid phase were negligible; (d) the interphase and intraparticle heat transfer resistances were negligible. The catalyst effectiveness factor equation for the hydrogenation of B_3D could be developed on the basis of the approaches already reported in the literature.[14,15] Under the conditions of significant

(12) Marquardt, D. W. *J. Sco. Ind. Appl. Math.* **1963**, *11*, 431.
(13) Tan, C. S.; Smith, J. M. *Chem. Eng. Sci.* **1980**, *35*, 1601
(14) Ramachandran, P. A.; Chaudhari, R. V. *Three Phase Catalytic Reactors*; Gordan and Breach: New York, 1983.
(15) Bischoff, K. B. *AIChE J.* **1965**, *11*, 351.

intraparticle gradient for the gas-phase reactant (H_2) and when the liquid-phase reactant was in excess, the overall rate of hydrogenation of B_3D was given as

$$R_A = \frac{\eta_C w k_1 A^* (B_l + k_{21} C_l)}{(1 + K_B B_l + K_c c)^2} \quad (4)$$

where η_C, the overall effectiveness factor for the spherical catalyst particle was given as

$$\eta_C = \frac{1}{\phi}\left(\coth 3\phi - \frac{1}{3\phi}\right) \quad (5)$$

ϕ is the Thiele parameter, and final dimensionless parameters are given in Appendix 1. For calculating ϕ, the values of effective diffusivity were estimated using the standard correlation.[15,16] Various correlations used to calculate the different coefficients in this work are given in Appendix 1. The saturation solubility of hydrogen was calculated as

$$(A^*)_T = [P - (P_V)_T](H_e)_T \quad (6)$$

where, P_v is the vapor pressure of solvent.

At steady-state conditions, the sum of the convection term and the gas−liquid mass transfer term were in equilibrium with the liquid−solid mass transfer term in the dynamic zone and the volumetric mass exchange between the dynamic and stagnant zone. The final mass balance equations in dimensionless form for species A (H_2) are given as

$$\frac{da_{ld}}{dz} = \alpha_{gl}(1 - a_{ld}) - \frac{\eta_C \alpha_r (b_l + k_{21} c_l)}{(1 + b_l k_b + c_l k_c)^2} x \left\{ \frac{f_d a_{ld}}{(1 + \eta_C \phi^2/N_d)} + \frac{f_s a_{ld}}{(1 + \eta_C \phi^2/N_s + \eta_c \phi^2/\alpha_s N_s)} \right\} \quad (7)$$

Similarly, the mass balance of liquid-phase reactant/products in dimensionless form can be given as

$$\frac{db_{l_d}}{dz} = -\frac{\eta_C \alpha_r b_l \chi}{q_B (1 + b_l k_b + c_l k_c)^2} \quad (8)$$

This equation represents the change in the concentration of B_3D in liquid phase in terms of dimensionless parameters.

$$\frac{dc_{l_d}}{dz} = \frac{\eta_C \alpha_r (b_l - k_{21} c_l) \chi}{q_B (1 + b_l k_b + c_l k_c)^2} \quad (9)$$

This equation represents the change in the concentration of B_2D in liquid phase in terms of dimensionless parameters.

$$\frac{dp_{l_d}}{dz} = \frac{\eta_C \alpha_r k_{21} c_l \chi}{q_B (1 + b_l k_b + c_l k_c)^2} \quad (10)$$

This equation represents the change in the concentration of B_1D in liquid phase in terms of dimensionless parameters, where

$$\chi = \left\{ \frac{f_d a_{ld}}{(1 + \eta_C \phi^2/N_\delta)} + \frac{f_s a_{ld}}{(1 + \eta_C \phi^2/N_s + \eta_C \phi^2/\alpha_s N_s)} + \frac{(1 - f_d - f_s) a_{ld}}{(1 + \eta_C \phi^2/N_g)} \right\} \quad (11)$$

A programe code in Q-Basic was developed to get the output of eqs 7−10. These equations were solved using a fourth-order Runge−Kutta method with the following initial conditions:

$$\text{At} \quad z = 0, \quad a_l = b_l = 1; \quad c_l = P_l = 0 \quad (12)$$

The model equations developed above, allowed the prediction of concentrations of products/reactants along the length of the reactor. At any given length of the reactor the fractional conversion of B_3D (X_B) could be given as

$$X_B = 1 - b_l \quad (13)$$

The overall rate of hydrogenation was calculated as

$$R_A = \frac{U_l}{L}(C_l + 2 P_l) \quad (14)$$

Here U_l, is the liquid velocity in m/s, L is the length of the catalyst bed in m, C_l, P_l are the concentrations of B_2D and B_1D, respectively. The selectivities of B_2D and B_1D were calculated as

$$S_{B_2D} = \frac{c_l}{(1 - b_l)} \times 100 \quad (15)$$

$$S_{B_1D} = \frac{P_l}{(1 - b_l)} \times 100 \quad (16)$$

The applicability of the model was verified by comparing the predicted concentration vs time profiles as well as conversion of B_3D and selectivities to B_2D and B_1D with the experimental results under various inlet conditions. These results have already been discussed above and are shown in Figures 5−8, which showed an excellent agreement between the predicted values and the experimental data.

Conclusions

Hydrogenation of 2-butyne-1,4-diol (B_3D) was carried out using 1% $Pt/CaCO_3$ catalyst in a fixed-bed reactor. This process represents a consecutive reaction scheme giving 2-butene-1,4- and butane-1,4-diols. In a continuous hydrogenation process, the ratio of butene- and butane diols could be manipulated by tailoring the operating conditions for the same catalyst. The liquid flow rate and pressure of the hydrogen gas showed a significant effect on the conversion

(16) Wilke, C. R.; Chang, P. *AIChE J.* **1955**, *1*, 246.
(17) Satterfield, C. N.; Way, P. F. *AIChE J.* **1972**, *18*, 305.
(18) Goto, S.; Smith, J. M. *AIChE J.* **1975**, *21*, 706.
(19) Satterfield, C. N.; Vab Eek, M. W.; Bliss, G. S. *AIChE J.* **1978**, *24*, 709.
(20) Zheng, L. P.; Smith, J. M.; Herskowitz, M. *AIChE J.* **1984**, *30*, 500.
(21) Hochmann, J. M.; Effron, E. *Ind. Eng. Chem. Fund.* **1969**, *8*, 63.
(22) Sato, Y.; Hiros, T.; Takahashi, F.; Toda, M. *J. Chem.. Eng. Japan* **1973**, *6*, 147.
(23) Zai-Sha, M.; Tian-Ying, X.; Chen, J. *Chem. Eng. Sci.* **1993**, *48*, 2697.
(24) Stephen, H.; Stephen, J. *Solubilities of Inorganic and Organic Compounds*; Pergamon Press: U.K. 1963; Vol. I, Part I.
(25) Mills, P. L.; Dudukovic, M. P. *AIChE J.* **1981**, *27*, 893.

of B_3D and overall rate of hydrogenation. A theoretical model was also developed incorporating the conditions of external and intraparticle mass transfer, partial wetting of the catalyst and reaction kinetics of butyne diol hydrogenation in a batch slurry reactor. The reactor model was validated by carrying out hydrogenation experiments under various reactor inlet conditions, and model predictions were found to agree well with the observed conversion, selectivity data.

NOTATION

a_l concentration of hydrogen in liquid phase, ($= A_l/A^*$), dimensionless

a_s concentration of hydrogen on the catalyst surface, ($= A_s/A^*$), dimensionless

a_p external surface area of the pellet [$= 6(1 - \epsilon_B)/d_P$], m^{-1}

a_t packing external surface area per unit volume of the reactor [$= S_{ex}(1 - \epsilon_b)/V_B$]

a_w catalyst area wetted, m^{-1}

A_l concentration of hydrogen in liquid phase, kmol/m^3

A_s concentration of hydrogen on the catalyst surface, kmol/m^3

A^* concentration of hydrogen in equilibrium with liquid, kmol/m^3

b_l concentration of B_3D in liquid phase ($= B_l/B_{li}$), dimensionless

B_l concentration of B_3D in liquid phase, kmol/m^3

B_{li} initial concentration of B_3D in liquid phase, kmol/m^3

c_l concentration of B_2D in liquid phase, ($= C_l/B_{li}$), dimensionless

C_l concentration of B_2D in liquid phase, kmol/m^3

D_e effective diffusivity, m^2/s

D_M molecular diffusivity, m^2/s

d_p particle diameter, m

f_d fraction of catalyst wetted by dynamic liquid

f_s fraction of catalyst wetted by the stagnant liquid

f_w wetted fraction

F liquid flow rate, kg/h

k_1, k_2 reaction rate constants, (m^3/kg) (m^3/kmol·s)

k_{21} dimensionless rate constant ($= k_2/k_1$)

k_b, k_c dimensionless equilibrium constant ($k_b = K_B B_{li}$; $k_c = K_C B_{li}$)

k_s liquid−solid mass transfer coefficient, m s^{-1}

k_{gs} gas-particle mass transfer coefficient, m s^{-1}

K_A, K_B, K_C adsorption constants, m^3/kmol

$k_l a_B$ gas−liquid mass transfer coefficient, s^{-1}

K_{ex} exchange coefficient between dynamic and stagnant liquid, s^{-1}

L reactor length, m

N_d Nusslet number for the liquid phase in the dynamic zone

N_s Nusslet number for the liquid phase in the stagnant zone

N_g Nusslet number for the gas phase

q_B stoichiometric ratio ($= B_{li}/A^*$)

r_1, r_2 reaction rate for the individual hydrogenation steps, kmol/m^3/s

R radius of the pellet, m

R_A overall rate of hydrogenation, kmol/m^3/s

Re_l Reynolds number for the liquid phase

S_{ex} external surface area of the catalyst pellet, m^2

U_g gas velocity (superficial), m/s

U_l liquid velocity (superficial), m/s

W weight of catalyst, kg/m^3

Z reactor length, *m*

Greek letters

α_{gl} dimensionless gas−liquid mass transfer coefficient

α_{ls} dimensionless liquid−solid mass transfer coefficient

α_r dimensionless reaction rate constant

ϵ porosity of catalyst

ϵ_b bed voidage

Appendix 1

(1) Dimensionless parameters used in the model:

gas−liquid mass transfer	$a_g = k_l\, a_B\, L/U_l$
liquid−solid mass transfer	$a_{ls} = k_S\, a_p\, L/U_l$
gas−solid mass transfer	$a_{gs} = k_{gs}\, a_p\, L/U_l$
Nusslet no. in dynamic zone	$N_d = R\, k_{sd}/3\, D_e$
Nusslet no. in stagnant zone	$N_S = R\, k_{Ss}/3\, D_e$
reaction rate constant	$\alpha_r = Lwk_l b_i/U_l$
equilibrium constants	$k_{21} = k_2/k_1$; $k_b = K_B\, B_l$; $k_C = K_C\, B_l$
Thiele parameter	$\phi = \frac{R}{3}\left[\frac{S_p(k_1 B_l + k_2 C_l)}{D_e(1 + K_B B_l + K_C C_l)^2}\right]^{1/2}$

(2) Correlations used in this work:

parameter	author(s)	ref
molecular diffusitivity	Wilke and Chang	16
gas−liquid mass transfer coefficient	Goto and Smith	18
liquid−solid mass transfer coefficient	Satterfield et al.(1978)	19
gas-particle mass transfer coefficient (value used)	Zheng Lu et al.	20
volumetric mass exchange coefficient	Hochmann and Effron	21
total liquid hold-up	Sato et al.	22
static liquid hold-up (value used)	Zai-sha Mao et al.	23
saturation solubility	Stephen and Stephen	24
wetting efficiency	Mills and Dudukovic	25

Received for review October 28, 2005.

OP050216R